

Multifractal Spin-Glass Chaos Projection and Interrelation of Multicultural Music and Brain Signals

E. Can Artun,¹ Ibrahim Keçoğlu,² Alpar Türkoğlu,^{2,3} and A. Nihat Berker^{1,4}

¹*Faculty of Engineering and Natural Sciences, Kadir Has University, Cibali, Istanbul 34083, Turkey*

²*Department of Physics, Boğaziçi University, Bebek, Istanbul 34342, Turkey*

³*Department of Electrical and Electronics Engineering,
Boğaziçi University, Bebek, Istanbul 34342, Turkey*

⁴*Department of Physics, Massachusetts Institute of Technology, Cambridge, Massachusetts 02139, USA*

A complexity classification scheme is developed from the fractal spectra of spin-glass chaos and demonstrated with multigeographic multicultural music and brain electroencephalogram signals. Systematic patterns are found to emerge. Chaos under scale change is the essence of spin-glass ordering and can be obtained, continuously tailor-made, from the exact renormalization-group solution of Ising models on frustrated hierarchical lattices. The music pieces are from Turkish music, namely Arabesque, Rap, Pop, Classical, and Western music, namely Blues, Jazz, Pop, Classical. A surprising group defection occurs.

I. INTRODUCTION: SPIN-GLASS CHAOS AS A COMPLEXITY CLASSIFICATION SCHEME

One beauty of complex systems from different sources is similar properties hidden under the complicated behaviors, waiting to be unveiled. [1, 2] On the other hand, "Chaos under scale change" as the distinctive characteristic of a spin-glass phase [3–6, 8–14] and the multifractal spectrum quantification of exceedingly complicated data can be merged to create a classification scheme for complex systems. In this scheme, the spin glasses can provide a standard metric for the wide range of complex systems. The connections of the thus classified complex systems could then be achieved, for example connecting different cultural trends, geographies, and time periods.

In the current work, we build such a complex-system classification scheme and illustrate its application with multicultural music and brain electroencephalogram (EEG) signals. Frozen microscopic disorder introduced into an ordering system can immediately: Completely eliminate [15] or reduce an ordered phase, change the critical exponents of a second-order phase transition [16, 17], convert a first-order phase transition into a second-order phase transition [18–21]. Competing microscopic interactions, with or without frozen microscopic disorder, furthermore can introduce a new phase, namely the spin-glass phase [22]. Competing microscopic interactions have two qualitatively different effects: (1) Two competing but non-cancelling (for example, due to unequal chain lengths) chains of interactions between two spatial points repress but do not eliminate the correlations. (2) On the other hand, if the local competing interactions cancel and create a local minimum energy degeneracy, correlations occur only in the form of the local configurations that participate into the degenerate local minimum energy. This effect is called frustration [23].

Hierarchical models [24–26] are exactly solvable microscopic models that are widely used.[27–35] The construction of a hierarchical model is illustrated in Fig.1(a)

[24]. The hierarchical lattice constructed in Ref.[3], for the study of competing interactions, included both the repression and frustration effects explained above. This construction is shown in Fig.1(b,c) and includes, in its basic graph, the specified indices of the number p_b of frustrated units, the number p of frustrating cross bonds, the number p_c of repressed units, the lengths $m_1, m_2 > m_1$ of the repressed chains.

Each line segment in Fig.1 represents a nearest-neighbor spin-spin interaction $J s_i s_j$, where at each site i of the lattice the Ising spin $s_i = \pm 1$. The Hamiltonian of the entire hierarchical lattice is

$$-\beta\mathcal{H} = J \sum_{\langle ij \rangle} s_i s_j, \quad (1)$$

where $\beta = 1/kT$ and $\langle ij \rangle$ denotes summation over all nearest-neighbor site pairs. The exact renormalization-group solution of the hierarchical model proceeds in the direction reverse to its construction (Fig.1), by summing over the internal spins shown with the dark circles. This summation yields the renormalization-group recursion relation $J' = J'(J)$, which becomes chaotic in wide ranges in the space of the indices $p, p_b, p_c, m_1, m_2 = m_1 + \Delta m$ chosen in the construction of the hierarchical model. Fig.2 shows the chaotic regions in cross sections of this multidimensional space of indices. Note islands that exclude chaos, such as the crescent and star region in the upper-right panel and all the lower panels in Fig.2. As explained in Ref.[3], chaotic renormalization-group trajectories signal the spin-glass phase, strong and weak correlations occurring in a random sequence at consecutive length scales and with extreme sensitivity to infinitesimal changes in external conditions such as temperature.[36] Chaotic renormalization-group trajectories and thus the spin-glass phase have subsequently been obtained in the approximate solution of systems with competing interactions, ferromagnetic versus antiferromagnetic interactions [37–39] or left-chiral versus right-chiral interactions [40–42], in cubic-lattice systems and re-wired [38] square-lattice systems.

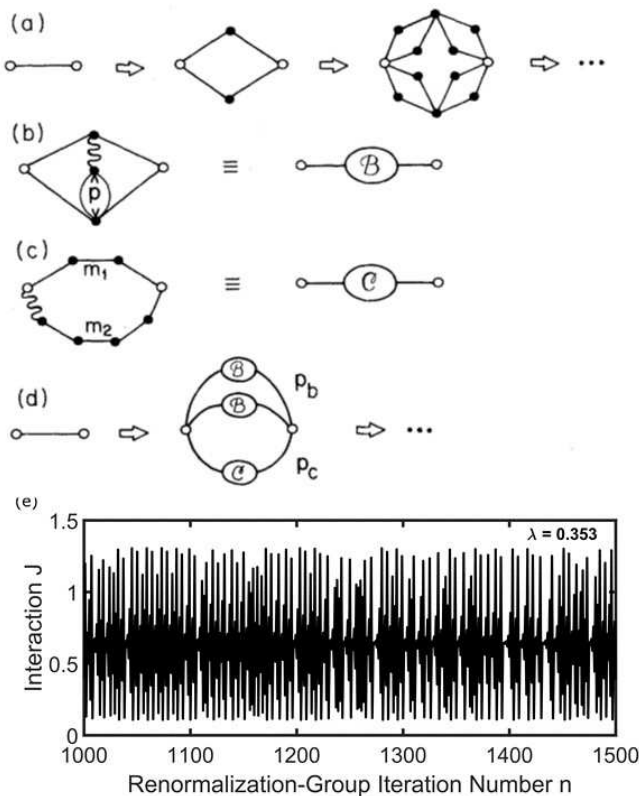


FIG. 1. Construction of the chaos hierarchical lattice, from Ref.[3]. (a) Construction of a standard hierarchical lattice, as explained in Ref.[24]. A graph is self-imbedded into each bond, *ad infinitum*. The exact renormalization-group solution proceeds in the reverse direction, by summing over the internal spins shown with the dark circles. In (b) and (c) are shown two graphs generic to the microscopics of spin glasses. The wiggly lines are infinite antiferromagnetic bonds, which have the sole effect of reversing the signs of the interactions adjoining on one side. (b) Frustrated units: Intermediate ferromagnetic (antiferromagnetic) ordering eliminates long-range antiferromagnetic (ferromagnetic) correlations. (c) Depressed units: The correlation on the shortest path sustains, but is depressed by the competing longer path. (d) Construction of the hierarchical lattice by combining the two generic units have yielded chaos in Ref.[3]. (e) A typical chaotic renormalization-group trajectory for this hierarchical lattice, *e.g.*, occurring for index values $p = 4, p_b = 40, p_c = 1, m_1 = 7, m_2 = m_1 + 1$. Each renormalization-group rescaling transformation is a renormalization-group iteration, here consecutively denoted by n . For a given set of indices, renormalization-group trajectories, starting at any temperature within the spin-glass phase, fall to the same chaotic trajectory. The Lyapunov exponent for the chaotic trajectory shown here is calculated (Eq.2) to be $\lambda = 0.353$. The Lyapunov exponents λ indicate the strength of chaos [7] and vary with the index values p, p_b, p_c, m_1, m_2 .

II. CHAOS UNDER SCALE CHANGE IN SPIN GLASSES: A CONTROLLABLE AND WIDE-RANGED BEHAVIOR FOR PROJECTION FROM COMPLEX SYSTEMS

Multifractal spectra are calculated for chaotic renormalization-group trajectories of the standard chaotic hierarchical lattice (Fig.1), music tracks from different geographies and cultural trends (Table I), brain EEG signals under different conditions, and, for future work, any complex system data set, as explained in Appendix A. For a given set of spin-glass indices p, p_b, p_c, m_1, m_2 , the starting temperature $T = J^{-1}$ of the chaotic renormalization-group trajectory is immaterial, as long as it is within the spin-glass phase, since a single chaotic trajectory is the asymptotic renormalization-group sink of the entire phase, attracting all initial conditions within the phase. For example, numerically identical Lyapunov exponents λ [43, 44], quantifying the strength of chaos, are obtained for all initial conditions inside the phase:

$$\lambda = \lim_{n \rightarrow \infty} \frac{1}{n} \sum_{k=0}^{n-1} \ln \left| \frac{dJ_{k+1}}{dJ_k} \right|, \quad (2)$$

where J_k is the value of the interaction constant in Eq.(1) after the k th renormalization-group transformation. Thus, our chaotic trajectories are taken after throwing out the first 1000 iterations and then using the next 2^{13} iterations, to eliminate transient effects of the crossover to the sink. In the examples shown in Fig.3, *e.g.*, we see that there is much stronger chaos in the music ($\lambda = 0.305$) than in the brain signals ($\lambda = 0.040$).

As shown in Fig.3, the spin-glass multifractal spectrum points are fitted by a continuous quartic function. The root-mean-square separation between the music (or brain EEG) multifractal spectrum points and the spin-glass continuous function is minimized by varying the original spin-glass indices of frustration number p_b and strand length m_1 . At the end of this procedure, the statistical correlation coefficient R_s between the spin-glass multifractal spectrum points and the spin-glass continuous function and the correlation coefficient R_m between the music multifractal spectrum points and spin-glass continuous function R_m together give the goodness of the fit between the spin-glass multifractal spectrum points and the music (or brain EEG) multifractal spectrum points. At the optimum fit, the calculated Lyapunov exponent λ measures the strength of the fitting chaos.[7]

III. CHAOTIC SPIN-GLASS CLASSIFICATION OF MULTICULTURAL AND MULTIGEORGAPHIC MUSIC

Scatter plots of the fitted frustrated hierarchical Ising models to multicultural music tracks are displayed in Fig. 4. Each point represents the fitted model indices for a single music track. There are ten tracks for each of the eight

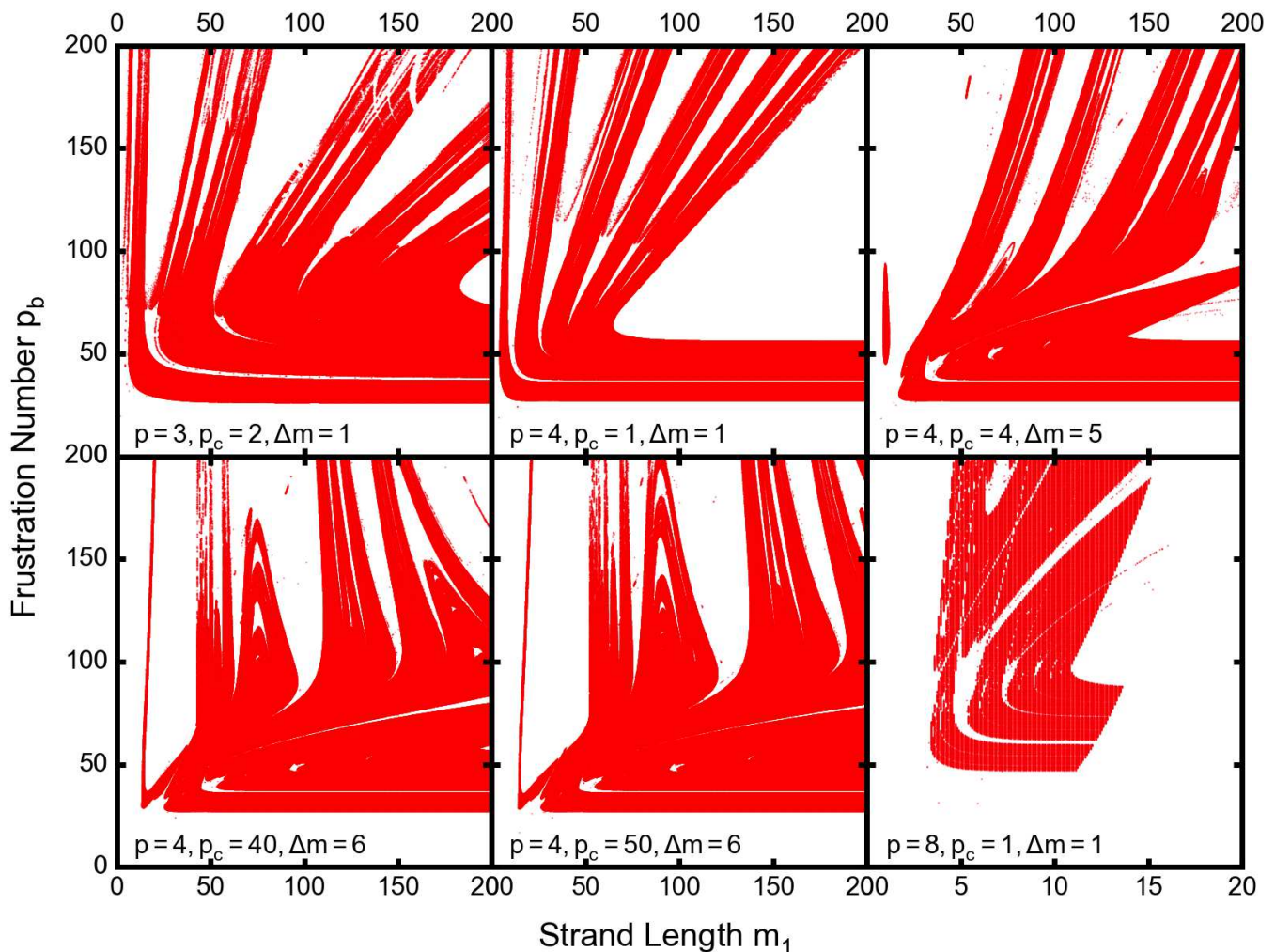


FIG. 2. Index regions of the frustrated hierarchical model that admit chaotic renormalization-group trajectories and, thus, a spin-glass phase. Note islands that exclude chaos, such as the crescent and star region in the upper-right panel and all the lower panels.

genres, separately listed in Table I. The genres are from Turkish music, namely Arabesque, Rap, Pop, Classical; and Western music, namely Blues, Jazz, Pop, Classical. In each panel, for the indicated values of p , p_c , Δm , the values of the frustration number p_b and repressed strand length m_1 are fitted to the music tracks. Thus, each panel is an alternate attempt to resolve the same data of 80 music tracks.

Systematic patterns emerge and are quite surprising. Firstly, essentially in all panels, the indices are organized in streaks that track each other. Blues, Jazz, and Western Classical (all from Western music), but not including Western Pop, stand apart. The other grouping is Turkish music (Arabesque, Rap, Pop, Classical), but also including Western Pop, all well mixed.

IV. CHAOTIC SPIN-GLASS CLASSIFICATION OF BRAIN EEG SIGNALS FROM DIFFERENTLY RESTING STATES AND CRANULAR REGIONS

Our calculated spin-glass multifractal indices for brain EEG signals, collected at different cranular probe locations and in the different states of music listening, resting with eyes open or closed, are displayed in Fig.5.[45–47] Again, an even clearer systematic pattern emerges. In the front cranular region, shown in the seven F panels, the indices fall on very well defined parallel streaks. There is predominant overlap between EEG signals from music listening and resting with eyes closed, as opposed to resting with eyes open. In the back cranular region, shown in the eight C panels, the separation is even clearer. For each panel, *i.e.*, each back cranular location, the spin-glass indices of the brain EEG data separate into two near-orthogonal branches. The horizontal branch, namely the

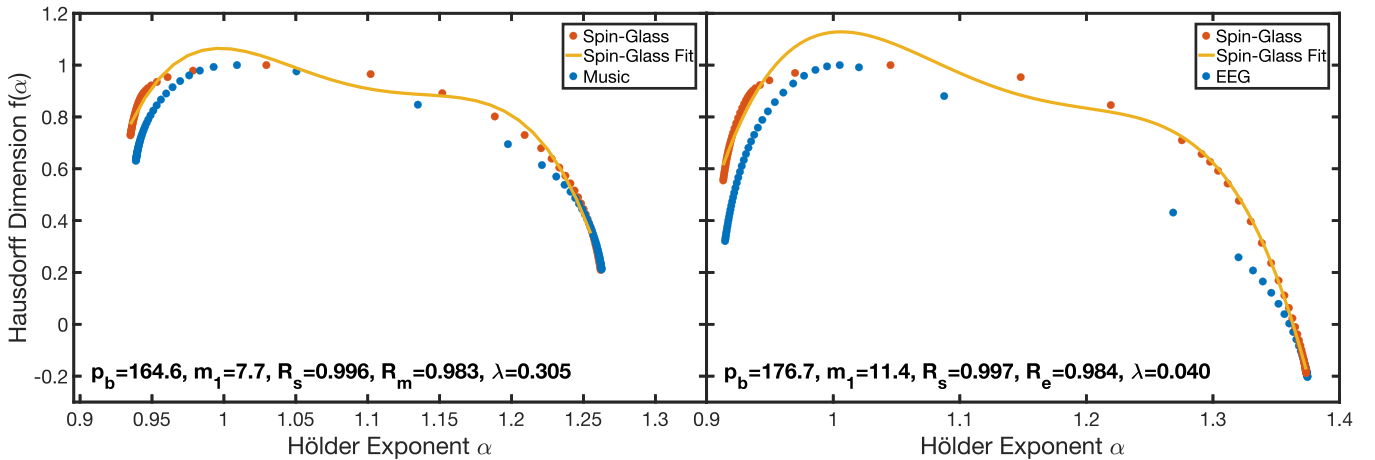


FIG. 3. Best fitting of SG multifractal spectrum points with the music spectrum (left panel) or brain EEG (right panel) points: The SG multifractal spectrum points are fitted by a continuous quartic function. The root-mean-square separation between the music or brain EEG spectrum points and the SG continuous function is minimized by varying the original spin-glass indices of frustration number p_b and repressed strand length m_1 . At the end of the procedure, the correlation coefficient R_s between the SG multifractal spectrum points and the SG continuous function, and the correlation coefficient R_m or R_e between the music spectrum or brain EEG points and SG continuous function R_m together give the goodness of the fit between the SG multifractal spectrum points and the music or brain EEG spectrum points. The calculated Lyapunov exponent λ measures the strength of the fitting chaos. In this figure, the multifractal SG music fit is illustrated with Bul Beni, Ezhel (Table I) in the left panel and the multifractal SG brain EEG fit with Music Listening, cranular location C_z (Fig.5) in the right panel.

constant (low) frustration number p_b branch, has the signals from music listening. The near-vertical branch, namely the near-constant (low) strand length m_1 , we find the EEG signals from music listening in its low p_b segment, then the EEG signals from resting with eyes closed in the upper segment, and the EEG signals from resting with eyes open clustered at the top p_b edge of the branch.

V. CONCLUSION

We have demonstrated that a complexity classification scheme can be developed from the fractal spectra of spin-glass chaos. We exemplified the procedure with 80 pieces multigeographic multicultural music from 8 genres and brain electroencephalogram signals. Systematic patterns and, in music, an interesting group defection is detected.

The tailor-made breadth and exact solution of spin-glass chaos makes this procedure a very widely usable classification and analysis scheme for all sorts of complex data.

ACKNOWLEDGMENTS

We thank Ratip Emin Berker and Deniz Eroğlu for very useful discussions and comments. Support by the Kadir Has University Doctoral Studies Scholarship Fund and by the Academy of Sciences of Turkey (TÜBA) is gratefully acknowledged.

Appendix A: Optimized Multifractal Sectra Fits between Chaotic Spin Glasses, Music, and Brain EEG

Two types of data have been used, the first of which is the experimental data (music or brain EEG) and the other is the chaotic spin-glass data, from the exact renormalization-group solution of the frustrated Ising model on a hierarchical lattice. We first fix the $p, p_c, \Delta m = m_2 - m_1$ values and do the renormalization-group transformation for each p_b and m_1 value between 0-200. While applying the renormalization-group transformations, we take 2^{13} iterations values after discarding the first 1000 iterations as crossover to asymptotic chaos. The occurrence of chaos for the given p_b and m_1 values is checked by calculating the Lyapunov exponent. For chaos, we apply Chhabra-Jensen Algorithm [49] to obtain the multifractal spectrum $f(\alpha)$ from the recurring J values. Thus, a repository of chaotic p_b and m_1 values and their correspondent $f(\alpha)$ is created to fit the music and brain EEG data.

To prepare the music data for Chhabra-Jensen algorithm, firstly the audio files have been transformed into time series data. We choose the left-ear channel in the time series. Then we discard the first 50000 data, which correspond mostly to silence, and take the next $2^{\lceil \log_2(N) \rceil}$ data, where N is the number of time series data points, because a power of 2 is needed in the Chhabra-Jensen algorithm. This data is normalized as $x'_i = (x_i - \tilde{x}_i)/\sigma_x$, where σ_x is the root-mean-square deviation of the data points and $\tilde{x}_i = 1/(1 + e^{x_i})$.

For the brain data, firstly the EEG data

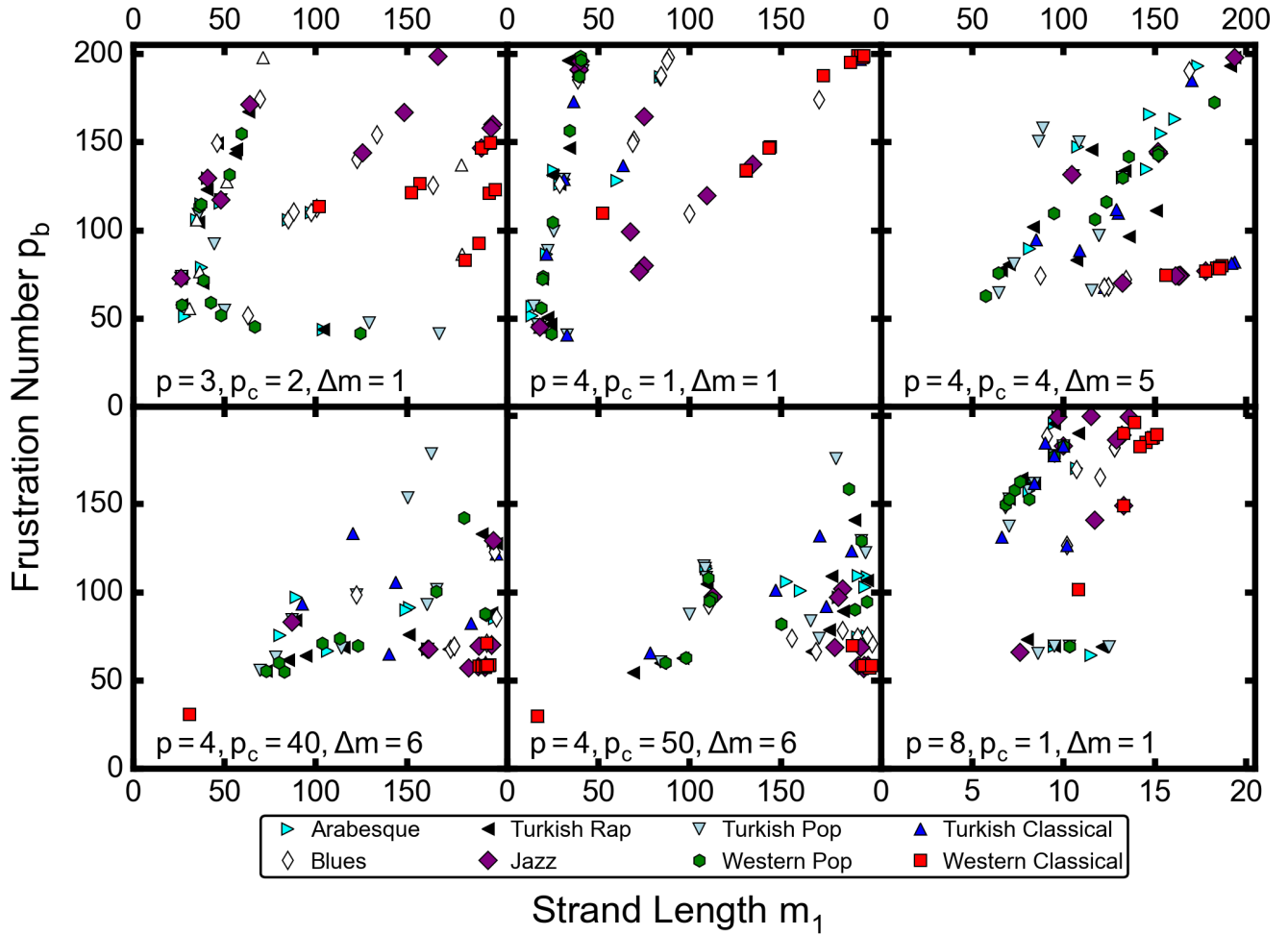


FIG. 4. Scatter plots of the fitted frustrated hierarchical Ising models to multicultural music tracks. Each point represents the fitted model indices for a single music track. There are ten tracks, listed in Table I, for each of the eight genres. In each panel, for the indicated values of $p, p_c, \Delta m$, the values of the frustration number p_b and repressed strand length m_1 are fitted to the music tracks. Systematic patterns emerge.

is imported to MATLAB(R2021a, The MathWorks, Inc., Natick) using FieldTrip Toolbox (<https://doi.org/10.1155/2011/156869>).[48] Then, a bandpass filter is applied, a common procedure when dealing with EEG data. To eliminate possible artifacts caused by the filtering, the first and last 3000 data points are discarded. Again, the first $2^{\lfloor \log_2(N) \rfloor}$ of the data is used and is normalized as described above.

Appendix B: Calculation of Multifractal Spectra of Chaotic Renormalization Group, Music, and Brain Signals

The Chhabra-Jensen function written by França *et al.* [49] is used, for all time-series data $A = \{a_1, a_2, \dots, a_N\}$ composed of N data points. Firstly, we split the data into disjoint sub-blocks $B_i = \{b_{i1}, b_{i2}, \dots, b_{il}\}$ of length l . Then we calculate the consecutive probabilities of each

block:

$$P_i(l) = \frac{\sum_{j=1}^l b_{ij}}{\sum_{j=1}^N a_j}. \quad (\text{B1})$$

We normalize the q th power of probabilities P_i and call it μ_i :

$$\mu_i(q, l) = \frac{P_i(l)^q}{\sum_j P_j(l)^q}. \quad (\text{B2})$$

Then we calculate the Hölder exponent α and the corresponding Hausdorff dimension $f(\alpha)$ to obtain the multifractal spectrum, by applying log-log fits to $M_\alpha(l)$ and $M_f(l)$:

$$\begin{aligned} M_\alpha(l) &= \sum_{i=1} \mu_i(q, l) \log_{10}(P_i(l)), \\ M_f(l) &= \sum_{i=1} \mu_i(q, l) \log_{10}(\mu_i(q, l)). \end{aligned} \quad (\text{B3})$$

The slopes found after regressing the log-log plots of $M_\alpha(l)$ and $M_f(l)$ are α and $f(\alpha)$. Repeating this fit for different q values, we obtain the multifractal spectrum.

-
- [1] D. Eroğlu, J. Lamb, S. W. Jeroen, and T. Pereira, Synchronisation of Chaos and its Applications, *Contemporary Phys.* **58**, 207 (2017).
- [2] D. Eroğlu, F. H. McRobie, I. Ozken, T. Stemler, K.H. Wyrwoll, S. F. M. Breitenbach, N. Marwan, and J. Kurths, See-Saw Relationship of the Holocene East Asian–Australian Summer Monsoon, *Nature Commun.* **7**, 1(2016).
- [3] S. R. McKay, A. N. Berker, and S. Kirkpatrick, Spin-Glass Behavior in Frustrated Ising Models with Chaotic Renormalization-Group Trajectories, *Phys. Rev. Lett.* **48**, 767 (1982).
- [4] S. R. McKay, A. N. Berker, and S. Kirkpatrick, Amorphously Packed, Frustrated Hierarchical Models: Chaotic Rescaling and Spin-Glass Behavior, *J. Appl. Phys.* **53**, 7974 (1982).
- [5] A. N. Berker and S. R. McKay, Hierarchical Models and Chaotic Spin Glasses, *J. Stat. Phys.* **36**, 787 (1984).
- [6] E. J. Hartford and S. R. McKay, Ising Spin-Glass Critical and Multicritical Fixed Distributions from a Renormalization-Group Calculation with Quenched Randomness, *J. Appl. Phys.* **70**, 6068 (1991).
- [7] S. E. Gürleyen and A.N. Berker, Asymmetric Phase Diagrams, Algebraically Ordered BKT Phase, and Peninsular Potts Flow Structure in Long-Range Spin Glasses, arXiv:2112.06258 [cond-mat.dis-nn] (2021).
- [8] Z. Zhu, A. J. Ochoa, S. Schnabel, F. Hamze, and H. G. Katzgraber, Best-Case Performance of Quantum Annealers on Native Spin-Glass Benchmarks: How Chaos Can Affect Success Probabilities, *Phys. Rev. A* **93**, 012317 (2016).
- [9] W. Wang, J. Machta, and H. G. Katzgraber, Bond Chaos in Spin Glasses Revealed through Thermal Boundary Conditions, *Phys. Rev. B* **93**, 224414 (2016).
- [10] L. A. Fernandez, E. Marinari, V. Martin-Mayor, G. Parisi, and D. Yllanes, Temperature Chaos is a Non-Local Effect, *J. Stat. Mech. - Theory and Experiment*, 123301 (2016).
- [11] A. Billoire, L. A. Fernandez, A. Maiorano, E. Marinari, V. Martin-Mayor, J. Moreno-Gordo, G. Parisi, F. Ricci-Tersenghi, J.J. Ruiz-Lorenzo, Dynamic Variational Study of Chaos: Spin Glasses in Three Dimensions, *J. Stat. Mech. - Theory and Experiment*, 033302 (2018).
- [12] W. Wang, M. Wallin, and J. Lidmar, Chaotic Temperature and Bond Dependence of Four-Dimensional Gaussian Spin Glasses with Partial Thermal Boundary Conditions, *Phys. Rev. E* **98**, 062122 (2018).
- [13] R. Eldan, The Sherrington-Kirkpatrick Spin Glass Exhibits Chaos, *J. Stat. Phys.* **181**, 1266 (2020).
- [14] M. Baity-Jesi, E. Calore, A. Cruz, L. A. Fernandez, J. M. Gil-Narvion, I. G.-A. Pemartin, A. Gordillo-Guerrero, D. Iñiguez, A. Maiorano, E. Marinari, V. Martin-Mayor, J. Moreno-Gordo, A. Muñoz-Sudupe, D. Navarro, I. Paga, G. Parisi, S. Perez-Gaviro, F. Ricci-Tersenghi, J. J. Ruiz-Lorenzo, S. F. Schifano, B. Seoane, A. Tarancon, R. Tripiccone, and D. Yllanes, Temperature Chaos Is Present in Off-Equilibrium Spin-Glass Dynamics, *Comm. Phys.* **4**, 74 (2021).
- [15] Y. Imry and S.-k. Ma, Random-Field Instability of Ordered State with Continuous Symmetry, *Phys. Rev. Lett.* **35**, 1399 (1975).
- [16] A. B. Harris, Effect of Random Defects on the Critical Behaviour of Ising Models, *J. Phys. C*, **7**, 1671 (1974).
- [17] D. Andelman and A. N. Berker, Scale-Invariant Quenched Disorder and its Stability Criterion at Random Critical Points, *Phys. Rev. B* **29**, 2630 (1984).
- [18] M. Aizenman and J. Wehr, Rounding of First-Order Phase Transitions in Systems with Quenched Disorder, *Phys. Rev. Lett.* **62**, 2503 (1989).
- [19] M. Aizenman and J. Wehr, *Phys. Rev. Lett.* **64**, 1311(E) (1990).
- [20] K. Hui and A. N. Berker, Random-Field Mechanism in Random-Bond Multicritical Systems, *Phys. Rev. Lett.* **62**, 2507 (1989).
- [21] K. Hui and A. N. Berker, erratum, *Phys. Rev. Lett.* **63**, 2433 (1989).
- [22] S.F. Edwards and P. W. Anderson, Theory of Spin Glasses, *J. Phys. F* **5**, 965 (1975).
- [23] G. Toulouse, Theory of Frustration Effect in Spin Glasses I., *Commun. Phys.* **2**, 115 (1977).
- [24] A. N. Berker and S. Ostlund, Renormalisation-Group Calculations of Finite Systems: Order Parameter and Specific Heat for Epitaxial Ordering, *J. Phys. C* **12**, 4961 (1979).
- [25] R. B. Griffiths and M. Kaufman, Spin Systems on Hierarchical Lattices: Introduction and Thermodynamic Limit, *Phys. Rev. B* **26**, 5022R (1982).
- [26] M. Kaufman and R. B. Griffiths, Spin Systems on Hierarchical Lattices: 2. Some Examples of Soluble Models, *Phys. Rev. B* **30**, 244 (1984).
- [27] A. V. Myshlyavtsev, M. D. Myshlyavtseva, and S. S. Akiemenko, Classical Lattice Models with Single-Node Interactions on Hierarchical Lattices: The Two-Layer Ising Model, *Physica A* **558**, 124919 (2020).
- [28] M. Derevyagin, G. V. Dunne, G. Mograby, and A. Teplyaev, Perfect Quantum State Transfer on Diamond Fractal Graphs, *Quantum Information Processing*, **19**, 328 (2020).
- [29] S.-C. Chang, R. K. W. Roeder, and R. Shrock, q-Plane Zeros of the Potts Partition Function on Diamond Hierarchical Graphs, *J. Math. Phys.* **61**, 073301 (2020).
- [30] C. Monthus, Real-Space Renormalization for Disordered Systems at the Level of Large Deviations, *J. Stat. Mech. - Theory and Experiment*, 013301 (2020).
- [31] O. S. Saryyer, Two-Dimensional Quantum-Spin-1/2 XXZ Magnet in Zero Magnetic Field: Global Thermodynamics from Renormalisation Group Theory, *Philos. Mag.* **99**, 1787 (2019).
- [32] P. A. Ruiz, Explicit Formulas for Heat Kernels on Diamond Fractals, *Comm. Math. Phys.* **364**, 1305 (2018).
- [33] M. J. G. Rocha-Neto, G. Camelo-Neto, E. Nogueira, Jr., and S. Coutinho, The Blume–Capel Model on Hierarchi-

- cal Lattices: Exact Local Properties, *Physica A* **494**, 559 (2018).
- [34] F. Ma, J. Su, Y. X. Hao, B. Yao, and G. G. Yan, A Class of Vertex–Edge-Growth Small-World Network Models Having Scale-Free, Self-Similar and Hierarchical Characters *Physica A* **492**, 1194 (2018).
- [35] S. Boettcher and S. Li, Analysis of Coined Quantum Walks with Renormalization, *Phys. Rev. A* **97**, 012309 (2018).
- [36] N. Aral and A. N. Berker, Chaotic Spin Correlations in Frustrated Ising Hierarchical Lattices, *Phys. Rev. B* **79**, 014434 (2009).
- [37] E. Ilker and A. N. Berker, High q-State Clock Spin Glasses in Three Dimensions and the Lyapunov Exponents of Chaotic Phases and Chaotic Phase Boundaries, *Phys. Rev. E* **87**, 032124 (2013).
- [38] E. Ilker and A. N. Berker, Overfrustrated and Underfrustrated Spin Glasses in $d=3$ and 2 : Evolution of Phase Diagrams and Chaos including Spin-Glass Order in $d=2$, *Phys. Rev. E* **89**, 042139 (2014).
- [39] E. Ilker and A. N. Berker, Odd q-State Clock Spin-Glass Models in Three Dimensions, Asymmetric Phase Diagrams, and Multiple Algebraically Ordered Phases, *Phys. Rev. E* **90**, 062112 (2014).
- [40] T. Çağlar and A. N. Berker, Chiral Potts Spin Glass in $d = 2$ and 3 Dimensions, *Phys. Rev. E* **94**, 032121 (2016).
- [41] T. Çağlar and A. N. Berker, Devil’s Staircase Continuum in the Chiral Clock Spin Glass with Competing Ferromagnetic-Antiferromagnetic and Left-Right Chiral Interactions, *Phys. Rev. E* **95**, 042125 (2017).
- [42] T. Çağlar and A. N. Berker, Phase Transitions Between Different Spin-Glass Phases and Between Different Chaoses in Quenched Random Chiral Systems, *Phys. Rev. E* **96**, 032103 (2017).
- [43] P. Collet and J.-P. Eckmann, *Iterated Maps on the Interval as Dynamical Systems* (Birkhäuser, Boston, 1980).
- [44] R. C. Hilborn, *Chaos and Nonlinear Dynamics*, 2nd ed. (Oxford University Press, New York, 2003).
- [45] M. Torkamani-Azar, S. D. Kanik, S. Aydın and M. Çetin, Prediction of Reaction Time and Vigilance Variability from Spatio-Spectral Features of Resting-State EEG in a Long Sustained Attention Task, *IEEE J. Biomedical and Health Informatics*, **24** 2550, (2020).
- [46] I. Daly, N. Nicolaou, D. Williams, F. Hwang, A. Kirke, E. Miranda, and S. J. Nasuto (2021), An EEG Dataset Recorded during Affective Music Listening, *OpenNeuro*, [Dataset] doi: 10.18112/openneuro.ds002721.v1.0.2 (2021).
- [47] P. Kraemer, *EEG* **10**, 20. Zenodo. <https://doi.org/10.5281/zenodo.3926093> (2020).
- [48] R. Oostenveld, P. Fries, E. Maris, and J.-M. Schoffelen, FieldTrip: Open Source Software for Advanced Analysis of MEG, EEG, and Invasive Electrophysiological Data, *Computational Intelligence Neuroscience* **2011**, e156869 (2010).
- [49] L. G. S. França, J. G. V. Miranda, M. Leite, N. K. Sharma, M. C. Walker, L. Lemieux, and Y. Wang, Fractal and Multifractal Properties of Electrographic Recordings of Human Brain Activity: Toward Its Use as a Signal Feature for Machine Learning in Clinical Applications, *Frontiers in Physiology* **9**, 01767 (2018).

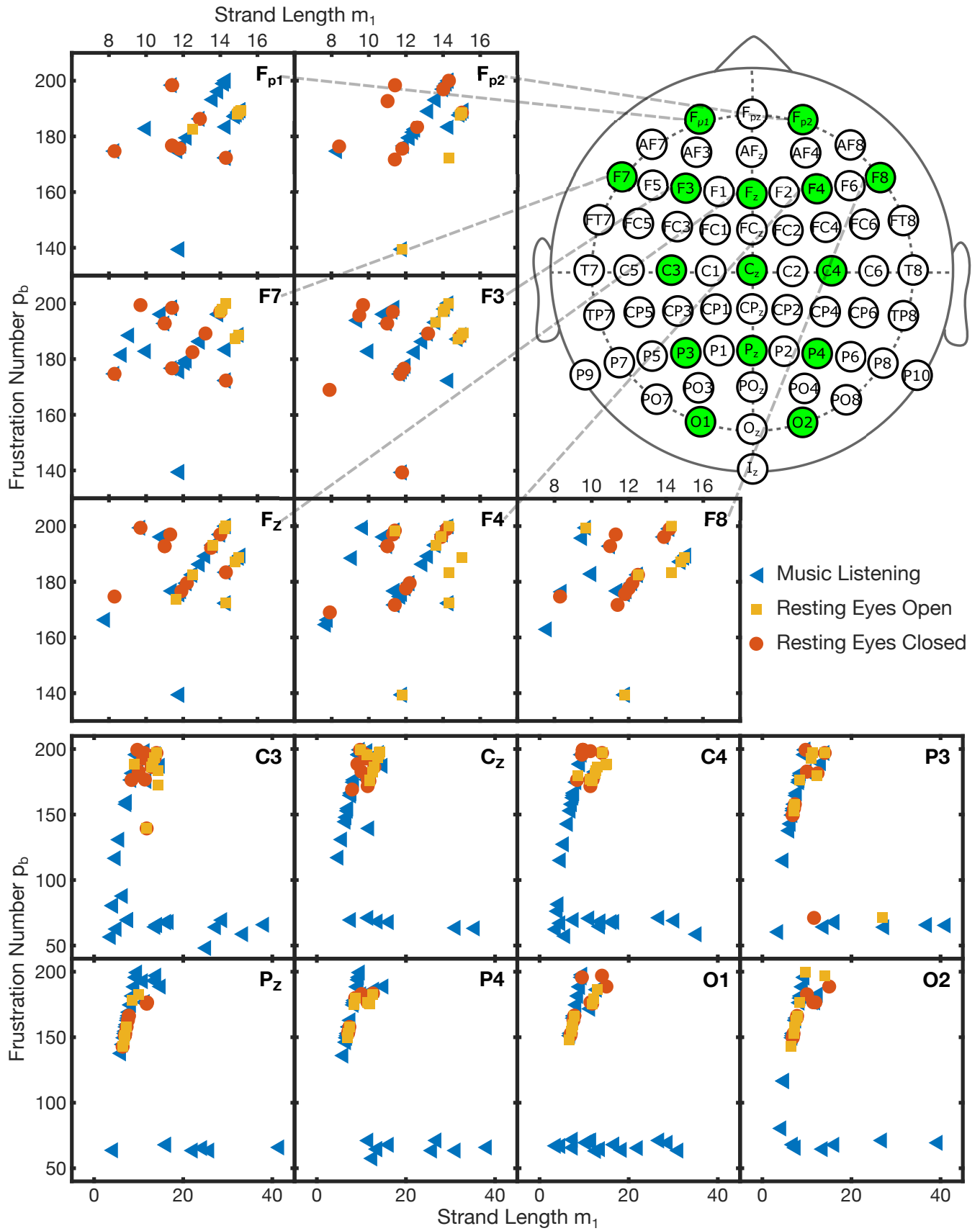


FIG. 5. SG multifractal parameters for EEG signals collected at different cranular probe locations, shown by the arrows, and in the different states of music listening, resting with eyes open or closed. Again, an even clearer systematic pattern emerges.

Composition, Artist	Composition, Artist
Arabesque	Blues
Elimde Duran Fotoğrafın, Bergen	Lonely Bed, Albert Cummings
Sev Yeter, Bergen	Lucille, B.B. King
Küllenen Aşk, Cengiz Kurtoğlu	She Is Crazy, Coldfire
Canma Okuyacağım, Ferdi Tayfur	The Sky Is Crying, Coleman
Vur Gitsin Beni, İbrahim Tathses	I Will Play the Blues for You, Daniel Castro
Bir Ateşe Attın, Kamuran Akkor	I'd Rather Go Blind, Etta James
Kadehi Şişeyi Kırarım Bugün, Kibariye	The Bluesbreakers John Mayall
Affet, Müslüm Gürses	Last Two Dollars, Johnnie Taylor
Unutamadım, Müslüm Gürses	Mannish Boy, Muddy Waters
Hatasız Kul Olmaz, Orhan Gencebay	Feeling Good, Nina Simone
Turkish Rap	Jazz
İzmir'in Ateşi, Ben Fero	Collard Greens Gand Black Eyed Peas, Bud Powell
Ben Ağlamazken, Ceza	More Today Than Yesterday, Charles Earland
Med Cezir, Ceza	Take Five, Dave Brubeck
Suspus, Ceza	Take The A Train, Duke Ellington
Zenti, Ex	Song For My Father, Horace Silver
Bul Beni, Ezhel	My Favorite Things, John Coltrane
Şehrmin Tadı, Ezhel	Una Mas, Kenny Dorham
Baytar, Sagopa Kajmer	The Sidewinder, Lee Morgan
Galiba, Sagopa Kajmer	Freddie Freeloader, Miles Davis
Makina, Uzi	So What, Miles Davis
Turkish Pop	Western Pop
Yerlerdeyim, Çelik	Hello, Adele
Bi Daha Bi Daha, Demet Akalın	Faded, Alan Walker
Bangır Bangır, Gülşen	Wake Me Up, Avicii
Sahte, Hande Yener	Favorito, Camilo
Sevgilim, Murat Boz	Woman, Doja Cat
Yoksa Yasak, Oğuzhan Koç	Photograph, Ed Sheeran
Poşet, Serdar Ortaç	Starving, Hailee Steinfeld
Şımarık, Tarkan	What Makes You Beautiful, One Direction
Ebruli, Yaşar	Let Her Go, Passenger
Kalbim Tatilde, Ziyet Sali	Closer, The Chainsmokers
Turkish Classical	Western Classical
Hicaz Ud Taksimi	Tocatta Och Fuga, Bach
Karciyar Kanun Taksimi	Piano Concerto Nr.5 Allegro, Beethoven
Kürdi Ud Taksimi	Minuet, Boccherini
Kürdilî Hicazkar Ud Taksimi	Hungarian Dances, Brahms
Muhayyer Kanun Taksimi	In The Hall of the Mountain King, Grieg
Nihavend Ud Taksimi	Ombra Mai Fu, Händel
Rast Ud Taksimi	Symphony Nr.40, Mozart
Saba Kanun Taksimi	Factotum Aria from Barber of Sevilla, Rossini
Suzinak Kanun Taksimi	Marche Militaire Nr.1, Schubert
Uşşak Kanun Taksimi	Piano Concerto No 1 B-Flat Minor, Tchaikovsky

TABLE I. Spin-glass-chaos indexed (Fig.4) multicultural music compositions by genre, title, and artist.